

# Tailoring the Crystallization Behavior and Mechanical Property of Poly(glycolic acid) by Self-nucleation

Jia-Xuan Li<sup>a</sup>, De-Yu Niu<sup>a</sup>, Peng-Wu Xu<sup>a\*</sup>, Zhao-Yang Sun<sup>b</sup>, Wei-Jun Yang<sup>a</sup>, Yang Ji<sup>b</sup>, and Pi-Ming Ma<sup>a\*</sup>

<sup>a</sup> The Key Laboratory of Synthetic and Biological Colloids, Ministry of Education, Jiangnan University, Wuxi 214122, China

<sup>b</sup> Inner Mongolia Pujing Polymer Material Technology Corporation Ltd., Baotou 014060, China

 Electronic Supplementary Information

**Abstract** Biocompostable poly(glycolic acid) (PGA) crystallizes slowly under fast cooling condition, leading to poor mechanical performance of the final products. In this work, a self-nucleation (SN) route was carried out to promote the crystallization of PGA by regulating only the thermal procedure without any extra nucleating agents. When self-nucleation temperature ( $T_s$ ) decreased from 250 °C to 227 °C, the nuclei density was increased, and the non-isothermal crystallization temperature ( $T_c$ ) of PGA was increased from 156 °C to 197 °C and the half-life time ( $t_{0.5}$ ) of isothermal crystallization at 207 °C was decreased by 89%. Consequently, the tensile strength and the elongation at break of the PGA were increased by 12% and 189%, respectively. According to the change of  $T_c$  as a function of  $T_s$ , a three-stage temperature domain map (Domain I, II and III) was protracted and the viscoelastic behavior of the self-nucleation melt and the homogeneous melt was studied. The results indicated that interaction among PGA chains was remained in Domain IIb, which can act as pre-ordered structure to accelerate the overall crystallization rate. This work utilizes a simple and effective SN method to regulate the crystallization behavior and the mechanical properties of PGA, which may broaden the application range of resulting materials.

**Keywords** Poly(glycolic acid); Self-nucleation; Crystallization kinetics; Mechanical property

**Citation:** Li, J. X.; Niu, D. Y.; Xu, P. W.; Sun, Z. Y.; Yang, W. J.; Ji, Y.; Ma, P. M. Tailoring the crystallization behavior and mechanical property of poly(glycolic acid) by self-nucleation. *Chinese J. Polym. Sci.* 2022, 40, 365–372.

## INTRODUCTION

It has become urgent to develop biodegradable polymers to prevent global plastic pollution from getting more and more serious.<sup>[1–4]</sup> Therefore, it is necessary to find degradable polymers as an alternative to non-degradable ones. Poly(glycolic acid) (PGA) is a new fully biodegradable and environmentally friendly polymer with high biocompatibility.<sup>[5]</sup> It can be degraded through soil burial, seawater and composting conditions, which will greatly alleviate environmental pressure. Compared with poly(lactic acid) (PLA), the most popular biodegradable polymer at the moment, PGA has higher mechanical strength, generally 80–120 MPa,<sup>[6]</sup> which enables PGA to be used in industries which require high(er) mechanical strength, such as fracturing plugs used in oil exploration. So far, surgical sutures<sup>[7]</sup> and tissue scaffolds<sup>[8]</sup> manufactured by PGA and its copolymers have been widely used because PGA can be completely metabolized by human body. In addition, PGA also has excellent gas barrier property making it potential in food packaging field.<sup>[6]</sup>

The advantages of PGA such as high mechanical strength and barrier property are related with its crystallization behavior and crystal structure. PGA generally possesses crystallinity as high as about 50%,<sup>[9]</sup> which is much higher than that of PLA. However, for processing such as film blowing and thin-wall injection molding, the crystallization rate of PGA is not high enough under rapid cooling condition. The low crystallinity influences the performance of PGA product massively, and thus the large-scale application is restricted.

To solve this problem, many methods have been used to enhance the crystallization rate of semi-crystalline polymers. Adding nucleating agents is the most popular and efficient method applied in processing and production. Nucleating agents mainly include inorganic nucleating agents,<sup>[10]</sup> macromolecular nucleating agents including stereocomplex (SC) crystallites,<sup>[11,12]</sup> and organic nucleating agents.<sup>[13,14]</sup> However, inorganic nucleating agents such as calcium carbonate usually require a larger amount of addition to achieve higher nucleation efficiency,<sup>[15]</sup> which will lead to a decrease in the mechanical properties. The nucleation effect of macromolecular nucleating agent is not always satisfying. For example, cellulose nanofiber was used as the macromolecular nucleating agent for PLA,<sup>[16]</sup> and crystallization temperature of PLA increased slightly. As for organic nucleating agents, orotic acid was used as an organic nucleating agent to induce the

\* Corresponding authors, E-mail: pengwuxu@jiangnan.edu.cn (P.W.X.)  
E-mail: p.ma@jiangnan.edu.cn (P.M.M.)

Received October 7, 2021; Accepted November 23, 2021; Published online January 20, 2022

crystallization of poly(3-hydroxybutyrate-co-3-hydroxyhexanoate) (PHBH).<sup>[17]</sup> The results showed that the crystallization time of PHBH with orotic acid was three times shorter than that with BN. Nevertheless, the organic nucleating agents require good lattice matching with the polymer. So far, there have been hardly any reports of high-efficiency organic nucleating agent suitable for PGA. Therefore, a universal method to increase the crystallization rate of PGA is needed.

Self-nucleation is also an effective method for increasing the crystallization rate by adjusting the thermal procedure of polymer crystallization, which is based on melt memory or crystal memory. In 1993, Fillon *et al.*<sup>[18]</sup> systematically studied self-nucleation phenomenon in isotactic polypropylene (*i*PP) system by means of differential scanning calorimetry (DSC) for the first time and provided the earliest study of self-nucleation thermal procedure. For decades, self-nucleation has been used in many semi-crystalline polymer systems to accelerate crystallization, *e.g.*, poly( $\epsilon$ -caprolactone) (PCL),<sup>[19]</sup> *i*PP,<sup>[20]</sup> and poly(butylene succinate) (PBS).<sup>[21]</sup> The relationship between self-nucleation effect and self-nucleation temperature,<sup>[22,23]</sup> annealing time,<sup>[24,25]</sup> molecular weight,<sup>[26,27]</sup> molecular chain confinement and topological structure<sup>[28,29]</sup> were studied in different polymer systems.

However, self-nucleation is mainly used in theoretical research, and the effect of self-nucleation on mechanical property is less studied<sup>[30]</sup> and there is hardly any work focusing on self-nucleation of PGA. In this work, the influence of self-nucleation effect on crystallization behavior, crystal morphology and mechanical properties of PGA is systematically studied, and the mechanism is further explored. This work utilized a simple and effective self-nucleation method to increase the crystallization rate and mechanical properties of PGA, and the output from this work could be very useful to the application of PGA as a general biodegradable material in the field of, *e.g.*, packaging.

## EXPERIMENTAL

### Materials

PGA ( $M_n=1.5 \times 10^5$  g/mol and  $M_w/M_n=1.3$ ) in the form of pellets was supplied by Shanghai Pujing Chemical Industry Co. Ltd., China.

### Sample Preparation

PGA pellets were dried at 80 °C under vacuum drying oven for 12 h before use. Then the pellets were hot compressed at 240 °C (for 1 min under 10 MPa) into sheets for further characterizations. In particular, the other hot compress temperatures for characterization of mechanical properties are described additionally in the next section.

### Characterization

#### Differential scanning calorimetry

DSC (Perkin Elmer DSC 8000, USA) was used to characterize the crystallization behavior of PGA under nitrogen atmosphere. The thermal procedure is illustrated in Fig. 1.

#### Non-isothermal crystallization

① Heating to a temperature which is 25–30 °C higher than the melting temperature ( $T_m$ ) of PGA (appr. 223 °C) to erase the crystalline memory. Specifically, heating from 50 °C to 260 °C at 50 °C/min and holding for 1 min to produce a homogeneous melt. ② Cooling to 0 °C at 10 °C/min to produce the standard crystallization state, as the same thermal history of all the samples. ③ Heating to different selected self-nucleation temperature ( $T_s$ ) at 10 °C/min, and holding at  $T_s$  for 5 min as the annealing time ( $t_s$ ). ④ Cooling to 0 °C at 10 °C/min, and finally ⑦ reheating to 260 °C at 10 °C/min.

#### Isothermal crystallization

Same as the thermal procedure of the non-isothermal crystallization, ① erasing crystalline history, ② creating a standard crystallization state and ③ heating to different  $T_s$  at 10 °C/min and holding for 5 min. Then ⑤ cooling to isothermal crystallization temperature rapidly at 50 °C/min, ⑥ holding for enough time to complete isothermal crystallization, and finally ⑦ reheating to 260 °C at 10 °C/min.

#### Polarized optical microscopy (POM)

Polarized optical microscopy (Axio Scope 1, Zeiss, Germany) with a hot stage (THMS600, Linkam, UK) was used to characterize the crystal morphology changes of PGA during non-isothermal crystallization at different  $T_s$ . Thermal procedure conducted in POM measurements is also illustrated in Fig. 1 (①②③④⑦).

#### Mechanical properties

Mechanical properties of PGA sheets ( $T_s=237$  °C and 260 °C)

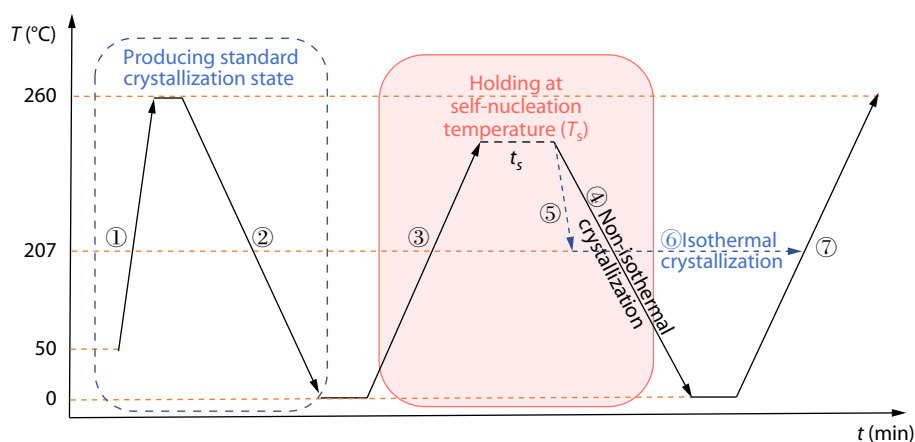


Fig. 1 Thermal procedure of PGA employed in the self-nucleation procedure.

were measured using a universal tester (Instron 5967, USA) according to G/BT 529-2008 at a crosshead speed of 10 mm/min. Five specimens of each sample were examined and the averaged values were presented. All the tests were performed at room temperature. The  $T_s$  was controlled by hot compress temperature (237 °C, 260 °C). Although the PGA pellets did not undergo erasing thermal history and crystallization process as ① and ② in Fig. 1, they were in the same thermal state before hot pressing, so the hot pressing temperature can be used as  $T_s$  under this condition.

#### Rheological behavior

Rheometer (Discovery DHR-2, TA instrument, USA) was used to characterize the dynamic rheological properties of PGA melts at different  $T_s$ s. The sample was heated to different  $T_s$ s (230–260 °C) after erasing crystalline history and producing standard crystallization state (similar to Fig. 1 ①②③). The samples were kept at selected  $T_s$  for 5 min, with a constant strain of 3% in a frequency-sweep mode (from 100 Hz to 0.01 Hz). The strain of 3% was pre-determined from a strain sweep experiment to make the measurements in a linear viscoelastic strain range.

## RESULTS AND DISCUSSION

### Influence of Self-nucleation Temperature on Non-isothermal Crystallization of PGA

The cooling and secondary heating DSC curves of PGA after holding 5 min at different  $T_s$ s are shown in Figs. 2(a) and 2(b), respectively. When  $T_s$  is above 250 °C, the crystallization temperature ( $T_c$ ) does not change significantly with  $T_s$ . When  $T_s$  decreases from 245 °C to 227 °C,  $T_c$  increases drastically from 164 °C to 197 °C. The crystallization peak changes from a broad peak to a sharp and narrow peak shape, indicating that self-nucleation at lower  $T_s$  induces PGA to crystallize more easily and the crystallization rate is faster during cooling. Therefore, self-nucleation has a significant effect on improving the crystallization rate of PGA.

From Fig. 2(b), it seems that when  $T_s$  is above 240 °C,  $T_s$  does not affect the  $T_m$  of PGA, and the melting peak is a single peak. However, when  $T_s$  decreases from 235 °C to 227 °C, a bimodal phenomenon appears in the melting curves. Bimodal phenomenon is very common in the melting curve of

crystalline polyester materials.<sup>[31]</sup> The reason of the bimodal phenomenon is that the thin part of lamellae crystals melts first as the low-temperature melting peak, and then undergoes melt-recrystallization to transform into thicker lamellae, which melt together with the original thick part and present as the high-temperature melting peak.

For this work, it may be explained that when  $T_s$  is higher than 250 °C, the crystallization of PGA is mainly driven by temperature to form the initial nuclei, so the crystallization process is almost the same as standard crystallization (process ② in Fig. 1). When  $T_s > 250$  °C, because there are fewer crystal nuclei, the growth space of spherulites is larger, and the crystals are relatively more complete with mainly thicker lamellae. During the secondary heating, the thinner lamellae recrystallize at about 200 °C, and reorganize into thicker lamellae and then melt together with the original thick lamellae. However, when  $223$  °C  $< T_s < 250$  °C, due to self-nucleation effect,  $T_c$  increases as  $T_s$  decreases, a large number of imperfect crystals with thin lamellae were formed quickly during the cooling process. These crystals melt first, leading to the appearance of melting double peaks.

It should be noted that when  $T_s = 223$  °C, which is close to the  $T_m$  of PGA, a high-temperature melting peak (227 °C) appears on the right side of the melting peak in the secondary heating curve. This is because there are crystal remnants that are not molten at a low  $T_s$ . This part undergoes high-temperature annealing at 223 °C, increasing the melting temperature. Meanwhile, the crystallinity at  $T_s = 223$  °C increases to 66.7% (Table S1 in the electronic supplementary information, ESI), which confirms the original crystals do not melt completely, but further thicken by high temperature annealing, thus the crystallinity and  $T_m$  increase.

### Influence of Self-nucleation Temperature on Non-isothermal Crystallization of PGA

In order to study the influence of annealing time on self-nucleation effect, 237 °C was selected as  $T_s$  and the annealing time was 1, 5, 10, 20 min, and the corresponding DSC results are shown in Fig. 3. Obviously,  $T_c$  basically remains unchanged with the increase of the annealing time. The result shows the stability of self-nucleation at a certain  $T_s$ , which can be affected by temperature other than annealing time. Stephanie *et al.*<sup>[32]</sup>

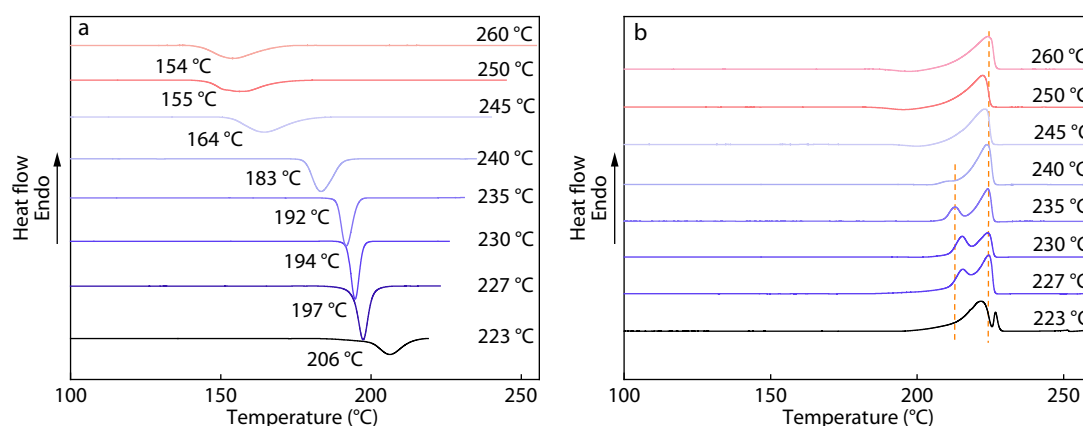


**Fig. 2** (a) Cooling (④ in Fig. 1) and (b) secondary heating (⑦ in Fig. 1) DSC curves of PGA at different  $T_s$ s (marked in the right side of each figure).

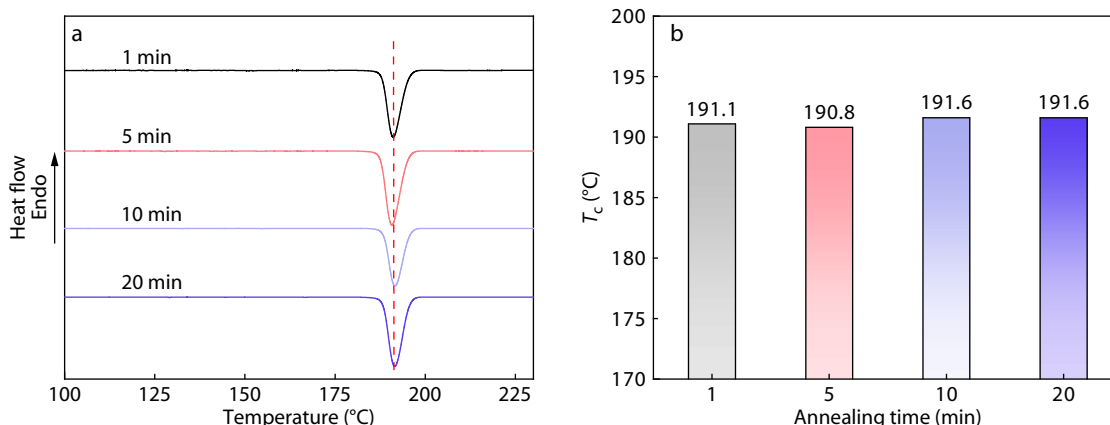


**Fig. 3** (a) DSC cooling curves of PGA at  $T_s=237$  °C under different annealing time and (b) the corresponding  $T_c$ .

found similar results in halogen-substituted polyethylene. Besides, Chen *et al.*<sup>[25]</sup> extended the annealing time to 1200 min in hydrogenated polybutadiene (HPB) system, and found that  $T_c$  only dropped by 1 °C. They also found that the activation energy for the disappearance of the self-nucleation effect was much higher than that for the dissolution of flow-induced nucleation, also verifying the self-nucleation stability.

#### Isothermal Crystallization of PGA Induced by Self-nucleation

Isothermal crystallization was carried out to further study the crystallization behaviors of PGA induced by self-nucleation. Fig. 4(a) shows the isothermal crystallization curves of PGA with different  $T_s$ s (227, 230, 235, 240 and 260 °C). PGA cannot crystallize at 207 °C with  $T_s=260$  °C within 40 min. When  $T_s$  decreases to 227 °C, PGA has finished the crystallization process within 10 min. The crystallization time decreases with the decrease of  $T_s$ . The half-life crystallization time ( $t_{0.5}$ ) is defined as the time required to reach 50% of the final crystallinity and the  $t_{0.5}$  of PGA with different  $T_s$ s is shown in Fig. 4(b). The  $t_{0.5}$  with  $T_s=227$  °C is only 4.19 min, which is much lower than that at higher  $T_s$ . These results indicate that self-nucleation can significantly reduce the crystallization time of PGA and increase the crystallization rate by regulating  $T_s$ , which are consistent with the non-isothermal crystallization results.

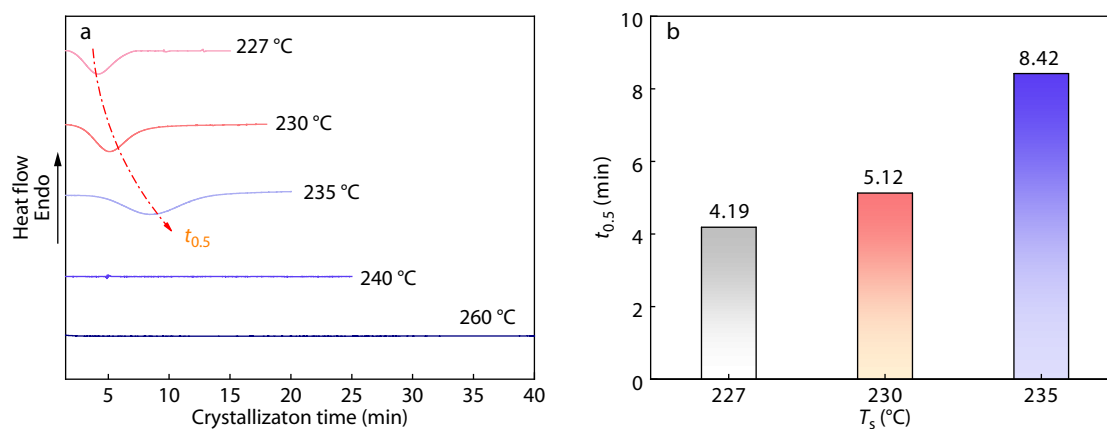


**Fig. 4** (a) DSC curves and (b) half-life crystallization time ( $t_{0.5}$ ) of isothermal crystallization of PGA at 207 °C with different  $T_s$ s (227, 230, 235, 240 and 260 °C)

#### Crystal Morphology

The effect of self-nucleation on the crystal morphology of PGA was characterized by POM and the results are displayed in Fig. 5. As shown in the left line of Fig. 5, when  $T_s=260$  °C, crystal nuclei appear at 206 °C and grow into regular spherulites with a radius of 77  $\mu\text{m}$  at 186 °C. Finally, the spherulites fill the entire view at 156 °C and the radius is more than 600  $\mu\text{m}$ . Such a large spherulite size can be a main reason of brittleness for PGA.<sup>[33,34]</sup> PGA could easily break along the smooth spherulitic boundary or the cracks formed in the spherulites, which greatly limits the application of PGA.

When  $T_s=237$  °C, in the right line of Fig. 5, the crystal morphology of PGA changes significantly. A huge number of small and dense granular crystals form very quickly, and fill the entire view as the temperature decreases. Compared with the crystal morphology of  $T_s=260$  °C, the self-nucleation effect greatly increases the crystal density and reduces the size of spherulites of PGA. From this phenomenon, it can be speculated that the change of crystal morphology may improve the brittleness of PGA.

#### Mechanism of PGA Self-nucleation

The above results have proved that self-nucleation can accelerate the crystallization of PGA by regulating  $T_s$ . The mechanism of fast crystallization induced by self-nucleation will



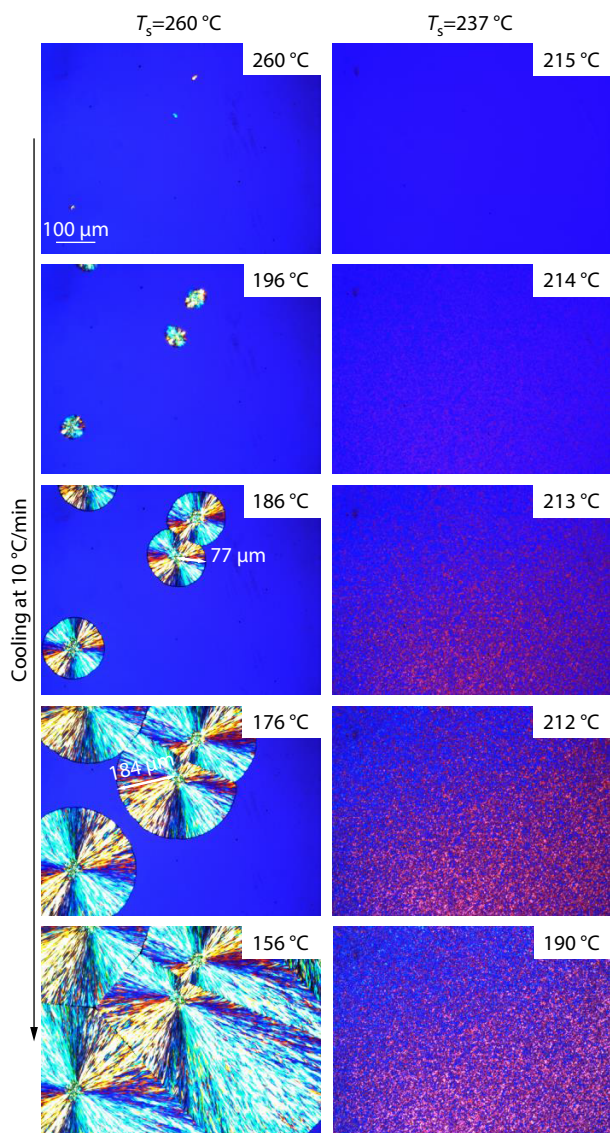


**Fig. 5** POM images of non-isothermal crystallization of PGA with  $T_s=237$  and  $260$  °C.

be discussed in detail. As shown in Fig. 6, we divided  $T_s$  into three zones (Domain I, Domain II and Domain III) and protracted a three-stage self-nucleation temperature domain map combining the characteristics of  $T_s$ ,  $T_c$  and the DSC melting curves of PGA.

Domain I ( $T_s > 250$  °C):  $T_c$  does not change with  $T_s$ . Domain II ( $223$  °C  $< T_s < 250$  °C):  $T_c$  increases significantly with the decrease of  $T_s$ . This domain can be subdivided<sup>[20]</sup> into Domain IIa ( $223$  °C  $< T_s < 227$  °C) and Domain IIb ( $227$  °C  $< T_s < 250$  °C), by the end of the PGA melting peak temperature,  $227$  °C. In Domain IIa, there are some small fragments crystals retain in the melt, and these fragments can induce the fast crystallization of PGA as nuclei. But lamellae thickening of crystals do not occur in Domain IIa. In Domain IIb, there are no fragments crystals in the melt because the  $T_s$  is higher than the end of the PGA melting peak temperature. However, there are still some molecular chains with ordered structures. These molecular chains can quickly assemble into nuclei to induce PGA crystal-

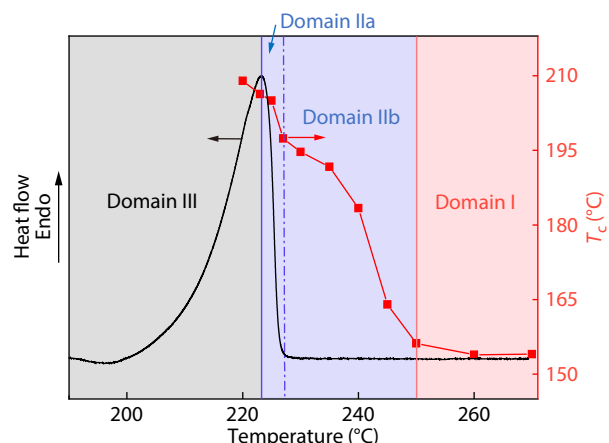


**Fig. 6**  $T_c$  of PGA as a function of  $T_s$  (red dotted line) superimposed on the melting endotherm (black line). The vertical blue and red lines mark the dividing temperatures between different domains.

lization, which will be discussed further in the following. Domain III ( $T_s < 223$  °C): the sign of this domain is the appearance of the high temperature annealing peak on the melting curve (Fig. 2b,  $T_s=223$  °C), indicating that there are crystals that have not molten during the 5 min annealing. After high temperature annealing, this part grows into thicker structure, thus obtaining higher melting temperature.

Recently, researchers used rheology measurements,<sup>[19,20]</sup> FTIR,<sup>[35]</sup> permittivity performance<sup>[36]</sup> and other methods for proving that specific interactions between polymer chains such as van der Waals force, dipole-dipole interaction, and hydrogen bonding interactions may be the origin of the melt memory effect. To figure out the nature of self-nucleation effect of PGA, rheological method was used to characterize the viscoelasticity of PGA melts at different  $T_s$ s and reveal the specific interactions that exist in SN melts.

The rheometer was used to measure the phase angle and complex modulus ( $G^*$ ) of PGA melt at different  $T_s$ s, in the linear viscoelastic region under small amplitude oscillating shear conditions. The relationship between phase angle and  $G^*$  is shown in Figs. 7(a) and 7(b).

Phase angle-complex modulus diagram is widely used in rheology, also called vGP graph, which is often used to characterize the compatibility of two phases in polymer blends.<sup>[37]</sup> The theory of this method is time-temperature superposition principle (TTS). For vGP plot, if the polymer melt obeys to TTS principle, the curves obtained at different temperatures should lie in the same curve, thus it can be considered as thermorheologically simple, otherwise is thermorheologically complex.

As can be seen in Figs. 7(a) and 7(b), in Domain IIb, the curves of phase angle and  $G^*$  cannot overlap, and the curves separate at high  $G^*$ ; while the curves of Domain I can overlap well. It reveals that the PGA melt of Domain I is thermorheologically simple and homogeneous; but the melt of Domain IIb is thermorheologically complex without obeying the TTS principle, and its heterogeneity can be confirmed. The origin of this heterogeneity is the nature of self-nucleation. Sangroniz *et al.*<sup>[19]</sup> used a similar method to plot the relationship between the phase angle and  $G^*$ , which proved the het-

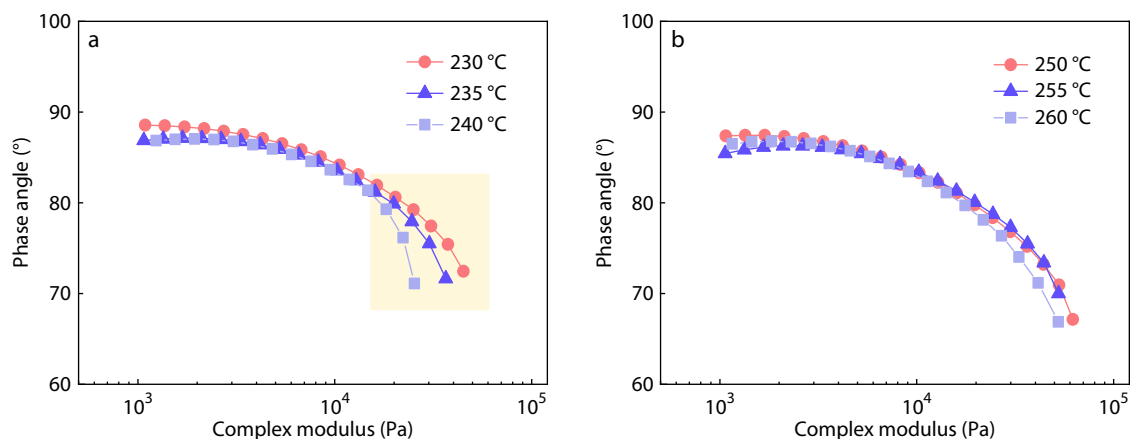


**Fig. 7** Phase angle as a function of the absolute value of complex modulus of PGA melt in (a) Domain IIb and (b) Domain I.

erogeneity of the SN melt.

Based on the above research, the mechanism of PGA self-nucleation effect can be summarized as follows (Fig. 8): (1) When  $T_s < 223$  °C, in Domain III, the unmolten crystals still exist in melt and undergo high temperature annealing and lamella thickening at  $T_s$ ; (2) When  $223$  °C  $< T_s < 227$  °C, in Domain IIa, some small fragments crystals or thicker lamellae<sup>[38]</sup> are retained in the melt, and serve as nuclei for epitaxial crystallization of PGA molecular chains when cooling, and accelerate the crystallization; (3) When  $227$  °C  $< T_s < 250$  °C, in Domain IIb, although the crystals melt completely and no crystal fragments exist, the interaction between molecular chains including van der Waals forces and dipole-dipole interactions is retained. This pre-ordered structure is the essence of the self-nucleation effect. The pre-ordered structure acts as “heterogeneous nuclei” to induce rapid recrystallization of PGA, also lowers the energy barrier for primary nucleation,<sup>[39]</sup> thus improves the crystallization of PGA; (4) When  $T_s > 250$  °C, in Domain I, the pre-ordered structure of the molecular chains is dissolved by heat, and the melt becomes homogeneous with thermorheologically simplicity, and thus self-nucleation effect vanishes.

### Mechanical Properties

For the moment, the researches on the self-nucleation effect on crystallization and its mechanism in various polymer systems. However, the effect of self-nucleation on the mechanical property of materials is relatively rarely studied. As a polymer with high mechanical strength, the mechanical strength of PGA is often concerned, so we studied the influence of self-nucleation on the mechanical properties of PGA.

Fig. 9(a) shows the tensile stress-strain curves of the PGA sample with  $T_s = 237$  and  $260$  °C. The comparison of the mechanical performance parameters is shown in Fig. 9(b) and Table S2 (in ESI). In addition, to eliminate the influence of crystallinity on mechanical properties, the crystallinity of samples with different  $T_s$ s was controlled at the same level, as shown in the Fig. S1 and Table S2 (in ESI). When  $T_s = 260$  °C, the tensile strength of PGA is 92.4 MPa, and the elongation at break is 4.6%; while when  $T_s = 237$  °C, the tensile strength and elongation at break are 103.9 MPa and 13.3%, respectively. Moreover, it can be observed that there is a tensile stress plateau with a certain increase of elongation in the tensile stress-strain curve of  $T_s = 237$  °C, which indicates the improvement of toughness by self-nucleation effect.

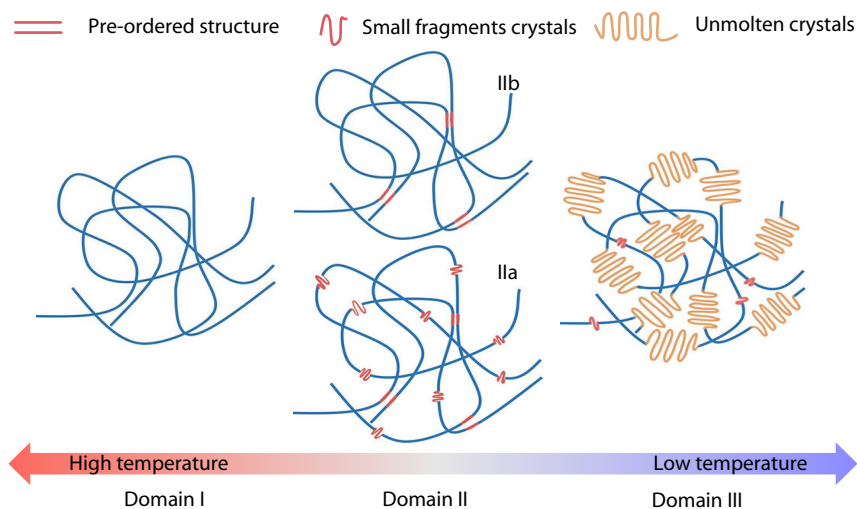


**Fig. 8** Schematic diagram of PGA melts in different domains.

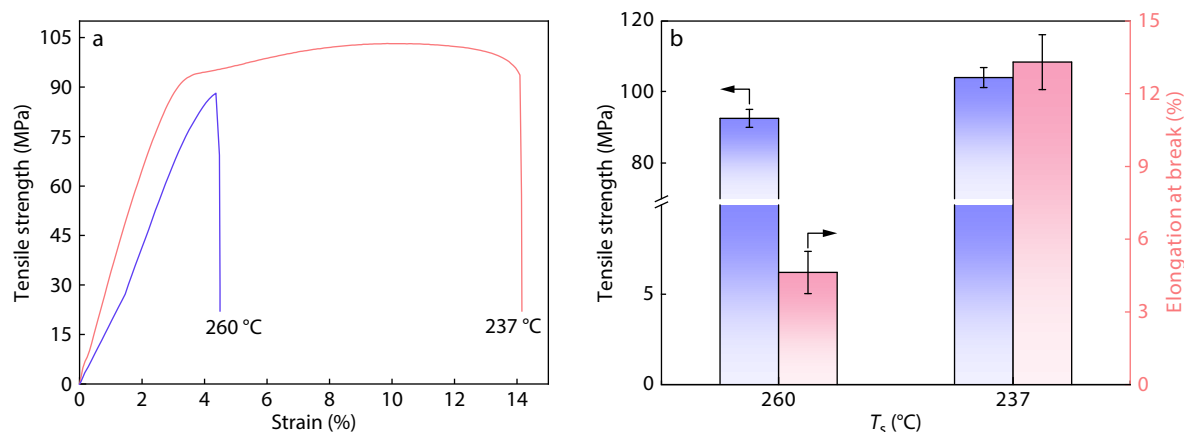


**Fig. 9** Effect of SN on mechanical properties of PGA (a) stress-strain curves (b) tensile strength and elongation at break.

The increase in toughness and strength is related to the change in morphology. When  $T_s$  is in Domain IIb, the nuclei density of PGA is larger and the crystal size is greatly reduced, in comparison with  $T_s$  in Domain I. Stress concentration is less likely to occur when the crystals are smaller and denser. Besides the tortuous crystalline boundary hinders the development of microcracks, leading to the improvement of toughness. In short, adjusting  $T_s$  can improve the tensile strength and toughness of PGA to a certain extent.

## CONCLUSIONS

This work utilized a self-nucleation route to improve the overall crystallization rate and mechanical performance of PGA. The crystallization temperature of PGA was increased from 154 °C to 197 °C, and  $t_{0.5}$  was decreased by 89.5% by regulating only the thermal procedure. The crystal size was decreased and nuclei density was increased significantly. As a consequence, the tensile strength and elongation at break of PGA were improved by 12.4% and 189.1%. Furthermore, the viscoelastic behaviors of the self-nucleation melt and the homogeneous melt were studied by rheological method. The results indicated that interaction among PGA chains was remained in Domain IIb, which can act as pre-ordered structure to accelerate the overall crystallization rate. Therefore, this work applied a simple SN method to improve the crystallization behavior and the mechanical properties of PGA, which may broaden the application range of resulting materials.

## NOTES

The authors declare no competing financial interest.

## Electronic Supplementary Information

Electronic supplementary information (ESI) is available free of charge in the online version of this article at <http://doi.org/10.1007/s10118-022-2671-y>.

## ACKNOWLEDGMENTS

This work was financially supported by the National Natural

Science Foundation of China (Nos. 51873082, 52073123 and 52103032), the Distinguished Young Natural Science Foundation of Jiangsu Province (No. BK20200027), and the Natural Science Foundation of Jiangsu Province (No. BK20200606).

## REFERENCES

- Wu, B.; Zeng, Q.; Niu, D.; Yang, W.; Dong, W.; Chen, M.; Ma, P. Design of supertoughened and heat-resistant PLLA/elastomer blends by controlling the distribution of stereocomplex crystallites and the morphology. *Macromolecules* **2019**, *52*, 1092–1103.
- Zhu, L.; Qiu, J.; Liu, W.; Sakai, E. Mechanical and thermal properties of rice straw/PLA modified by nano attapulgite/PLA interfacial layer. *Compos. Commun.* **2019**, *13*, 18–21.
- Georgiopoulos, P.; Kontou, E.; Georgousis, G. Effect of silane treatment loading on the flexural properties of PLA/flax unidirectional composites. *Compos. Commun.* **2018**, *10*, 6–10.
- Wu, B.; Yang, W.; Niu, D.; Dong, W.; Chen, M.; Liu, T.; Du, M.; Ma, P. Stereocomplexed poly(lactide) composites toward engineering plastics with superior toughness, heat resistance and anti-hydrolysis. *Chinese J. Polym. Sci.* **2020**, *38*, 1107–1116.
- Zhang, J.; Yang, S.; Yang, X.; Xi, Z.; Zhao, L.; Cen, L.; Lu, E.; Yang, Y. Novel fabricating process for porous polyglycolic acid scaffolds by melt-foaming using supercritical carbon dioxide. *ACS Biomater. Sci. Eng.* **2017**, *4*, 694–706.
- Yamane, K.; Sato, H.; Ichikawa, Y.; Sunagawa, K.; Shigaki, Y. Development of an industrial production technology for high-molecular-weight polyglycolic acid. *Polym. J.* **2014**, *46*, 769–775.
- Belenkaya, B. G.; Sakharova, V. I.; Sinevich, E. A.; Belousov, S. I.; Kuptsov, A. H.; Chvalun, S. N. Kinetics and mechanism of biodegradation of (co)polyglycolide sutures. *Macromol. Symp.* **2015**, *144*, 187–199.
- Oca, H.; Farrar, D. F.; Ward, I. M. Degradation studies on highly oriented poly(glycolic acid) fibres with different lamellar structures. *Acta Biomater.* **2010**, *7*, 1535–1541.
- Yu, C.; Bao, J.; Xie, Q.; Shan, G.; Bao, Y.; Pan, P. Crystallization behavior and crystalline structural changes of poly(glycolic acid) investigated via temperature-variable WAXD and FTIR analysis. *CrystEngComm* **2016**, *18*, 7894–7902.
- Xu, P.; Cui, Z.; Ruan, G.; Ding, Y. Enhanced crystallization kinetics of PLLA by ethoxycarbonyl ionic liquid modified graphene. *Chinese J. Polym. Sci.* **2019**, *37*, 243–252.
- Jiang, L.; Shen, T.; Xu, P.; Zhao, X.; Li, X.; Dong, W.; Ma, P.; Chen, M.

- Crystallization modification of poly(lactide) by using nucleating agents and stereocomplexation. *e-Polymers* **2016**, *16*, 1–13.
- 12 Wang, M.; You, L.; Guo, Y.; Jiang, N.; Gan, Z.; Ning, Z. Enhanced crystallization rate of poly(L-lactide)/hydroxyapatite-graft-poly(D-lactide) composite with different processing temperatures. *Chinese J. Polym. Sci.* **2020**, *38*, 599–610.
  - 13 Teng, S.; Jiang, Z.; Qiu, Z. Crystallization behavior and dynamic mechanical properties of poly( $\epsilon$ -caprolactone)/octaisobutyl-polyhedral oligomeric silsesquioxanes composites prepared via different methods. *Chinese J. Polym. Sci.* **2020**, *38*, 158–163.
  - 14 Xu, P.; Ma, P.; Cai, X.; Song, S.; Zhang, Y.; Dong, W.; Chen, M. Selectively cross-linked poly(lactide)/ethylene-glycidyl methacrylate-vinyl acetate thermoplastic elastomers with partial dual-continuous network-like structures and shape memory performances. *Eur. Polym. J.* **2016**, *84*, 1–12.
  - 15 Bosq, N.; Aht-Ong, D. Isothermal and non-isothermal crystallization kinetics of poly(butylene succinate) with nanoprecipitated calcium carbonate as nucleating agent. *J. Therm. Anal. Calorim.* **2018**, *132*, 233–249.
  - 16 Shazleen, S. S.; Yasimanuar, T.; Ibrahim, N. A.; Hassan, M. A.; Ariffin, H. Functionality of cellulose nanofiber as bio-based nucleating agent and nano-reinforcement material to enhance crystallization and mechanical properties of polylactic acid nanocomposite. *Polymers* **2021**, *13*, 389.
  - 17 Jacquél, N.; Tajima, K.; Nakamura, N.; Miyagawa, T.; Pan, P.; Inoue, Y. Effect of orotic acid as a nucleating agent on the crystallization of bacterial poly(3-hydroxybutyrate-co-3-hydroxyhexanoate) copolymers. *J. Appl. Polym. Sci.* **2010**, *114*, 1287–1294.
  - 18 Fillon, B.; Wittmann, J. C.; Lotz, B.; Thierry, A. Self-nucleation and recrystallization of isotactic polypropylene ( $\alpha$  phase) investigated by differential scanning calorimetry. *J. Polym. Sci., Part B: Polym. Phys.* **1993**, *31*, 1383–1393.
  - 19 Sangroniz, L.; Barbieri, F.; Cavallo, D.; Santamaria, A.; Alamo, R. G.; Müller, A. J. Rheology of self-nucleated poly( $\epsilon$ -caprolactone) melts. *Eur. Polym. J.* **2018**, *99*, 495–503.
  - 20 Sangroniz, L.; Cavallo, D.; Santamaria, A.; Müller, A. J.; Alamo, R. G. Thermorheologically complex self-seeded melts of propylene-ethylene copolymers. *Macromolecules* **2017**, *50*, 642–651.
  - 21 Jiang, J.; Zhuravlev, E.; Hu, W.; Schick, C.; Zhou, D. The effect of self-nucleation on isothermal crystallization kinetics of poly(butylene succinate) (PBS) investigated by differential fast scanning calorimetry. *Chinese J. Polym. Sci.* **2017**, *35*, 1009–1019.
  - 22 Lorenzo, A. T.; Arnal, M. L.; Sánchez, J.; Müller, A. J. Effect of annealing time on the self-nucleation behavior of semicrystalline polymers. *J. Polym. Sci., Part B: Polym. Phys.* **2006**, *44*, 1738–1750.
  - 23 Hu, D.; Ye, S.; Yu, F.; Feng, J. Further understanding on the three domains of isotactic polypropylene by investigating the crystalline morphologies evolution after treatment at different domains. *Chinese J. Polym. Sci.* **2016**, *34*, 344–358.
  - 24 Michell, R. M.; Mugica, A.; Zubitur, M.; Müller, A. J. in *Polymer Crystallization I*, Springer, Germany, **2015**, p. 215.
  - 25 Chen, X.; Qu, C.; Alamo, R. G. Effect of annealing time and molecular weight on melt memory of random ethylene 1-butene copolymers. *Polym. Int.* **2018**, *68*, 248–256.
  - 26 Reid, B. O.; Vadlamudi, M.; Mamun, A.; Janani, H.; Gao, H.; Hu, W.; Alamo, R. G. Strong memory effect of crystallization above the equilibrium melting point of random copolymers. *Macromolecules* **2013**, *46*, 6485–6497.
  - 27 Pérez, R.; Córdova, M.; López, J.; Hoskins, J. N.; Müller, A. J. Nucleation, crystallization, self-nucleation and thermal fractionation of cyclic and linear poly( $\epsilon$ -caprolactone)s. *React. Funct. Polym.* **2013**, *80*, 71–82.
  - 28 Luo, C.; Sommer, J. U. Frozen topology: entanglements control nucleation and crystallization in polymers. *Phys. Rev. Lett.* **2014**, *112*, 195702.
  - 29 Pan, Y.; Yu, X.; Shi, T.; An, L. Nucleation and crystallization of H-shaped (PS)<sub>2</sub>PEG(PS)<sub>2</sub> block copolymers. *Chinese J. Polym. Sci.* **2010**, *28*, 347–355.
  - 30 Sangroniz, L.; Cavallo, D.; Müller, A. J. Self-nucleation effects on polymer crystallization. *Macromolecules* **2020**, *53*, 4581–4604.
  - 31 Shen, T.; Xu, Y.; Cai, X.; Ma, P.; Dong, W.; Chen, M. Enhanced crystallization kinetics of poly(lactide) with oxalamide compounds as nucleators: effect of spacer length between the oxalamide moieties. *RSC Adv.* **2016**, *6*, 48365–48374.
  - 32 Marxsen, S. F.; Alamo, R. G. Melt-memory of polyethylenes with halogen substitution: random vs. precise placement. *Polymer* **2019**, *168*, 168–177.
  - 33 Liu, S.; Yang, J.; Liu, Q.; Huang, Y.; Kong, M.; Yang, Q.; Li, G. Polydopamine particles as a  $\beta$ -nucleating agent and antioxidant for isotactic polypropylene. *Chem. Eng. J.* **2019**, *363*, 1–12.
  - 34 Hobbs, J. K.; McMaster, T. J.; Miles, M. J.; Barham, P. J. Cracking in spherulites of poly(hydroxybutyrate). *Polymer* **1996**, *37*, 3241–3246.
  - 35 Liu, X.; Wang, Y.; Wang, Z.; Cavallo, D.; Müller, A. J.; Zhu, P.; Zhao, Y.; Dong, X.; Wang, D. The origin of memory effects in the crystallization of polyamides: Role of hydrogen bonding. *Polymer* **2020**, *188*, 122117.
  - 36 Sangroniz, L.; Alamo, R. G.; Cavallo, D.; Santamaria, A.; Müller, A. J.; Alegria, A. Differences between isotropic and self-nucleated PCL melts detected by dielectric experiments. *Macromolecules* **2018**, *51*, 3663–3671.
  - 37 Liang, H.; Hao, Y.; Bian, J.; Zhang, H.; Dong, L.; Zhang, H. Assessment of miscibility, crystallization behaviors, and toughening mechanism of polylactide/acrylate copolymer blends. *Polym. Eng. Sci.* **2015**, *55*, 386–396.
  - 38 Li, J.; Jiang, Z.; Qiu, Z. Isothermal melt crystallization kinetics study of cellulose nanocrystals nucleated biodegradable poly(ethylene succinate). *Polymer* **2021**, *227*, 123869.
  - 39 Mamun, A.; Umamoto, S.; Okui, N. Self-seeding effect on primary nucleation of isotactic polystyrene. *Macromolecules* **2007**, *40*, 6296–6303.